*Protein Science* (1996), *5*:1662–1675. Cambridge University Press. Printed in the USA.


# Conformation and molecular topography of the N-terminal segment of surfactant protein B in structure-promoting environments

LARRY M. GORDON,[1] SUZANNA HORVATH,[2] MARJORIE L. LONGO,[3] JOSEPH A.N. ZASADZINSKI,[4] H. WILLIAM TAEUSCH,[5] KYM FAULL,[6] CAROL LEUNG,[1] AND ALAN J. WARING[1]

[1] Department of Pediatrics, Martin Luther King Jr./Charles R. Drew University Medical Center and Perinatal Laboratories, Harbor-University of California Los Angeles Medical Center, Los Angeles, California 90059
[2] Biopolymer Synthesis Center, Division of Biology, California Institute of Technology, Pasadena, California 91125
[3] Department of Chemical Engineering and Materials Science, University of California, Davis, Davis, California 95616
[4] Department of Chemical and Nuclear Engineering, University of California, Santa Barbara, California 93106
[5] Department of Pediatrics, San Francisco General Hospital/UCSF San Francisco, California 94110
[6] Center for Molecular and Medical Sciences Mass Spectrometry, Departments of Psychiatry and Biobehavioral Sciences, and Chemistry and Biochemistry, and Neuropsychiatric Institute, UCLA, Los Angeles, California 90024

(RECEIVED December 5, 1995; ACCEPTED May 21, 1996)

**Abstract**

Although the effects of surfactant protein B (SP-B) on lipid surface activity in vitro and in vivo are well known, the relationship between molecular structure and function is still not fully understood. To further characterize protein structure-activity correlations, we have used physical techniques to study conformation, orientation, and molecular topography of N-terminal SP-B peptides in lipids and structure-promoting environments. Fourier transform infrared (FTIR) and CD measurements of SP-$B_{1-25}$ (residues 1–25) in methanol, SDS micelles, egg yolk lecithin (EYL) liposomes, and surfactant lipids indicate the peptide has a dominant helical content, with minor turn and disordered components. Polarized FTIR studies of SP-$B_{1-25}$ indicate the long molecular axis lies at an oblique angle to the surface of lipid films. Truncated peptides were similarly examined to assign more accurately the discrete conformations within the SP-$B_{1-25}$ sequence. Residues Cys-8–Gly-25 are largely $\alpha$-helix in methanol, whereas the N-terminal segment Phe-1–Cys-8 had turn and helical propensities. Addition of SP-$B_{1-25}$ spin-labeled at the N-terminal Phe (i.e., SP-$B^{*}_{1-25}$) to SDS, EYL, or surfactant lipids yielded electron spin resonance spectra that reflect peptide bound to lipids, but retaining considerable mobility. The absence of characteristic radical broadening indicates that SP-$B_{1-25}$ is minimally aggregated when it interacts with these lipids. Further, the high polarity of SP-$B_{1-25}$ argues that the reporter on Phe-1 resides in the headgroup of the lipid dispersions. The blue-shift in the endogenous fluorescence of Trp-9 near the N-terminus of SP-$B_{1-25}$ suggests that this residue also lies near the lipid headgroup. A summary model based on the above physical experiments is presented for SP-$B_{1-25}$ interacting with lipids.

**Keywords:** CD spectroscopy; ESR spectroscopy; fluorescence; FTIR spectroscopy; lipid–peptide interactions; N-terminal domain; surfactant protein B

Reprint requests to: Alan J. Waring, Research and Educational Institute, Inc., Bldg. RB-1, 1124 W. Carson Street, Torrance, California 90502-2064; e-mail: awaring@meded.com.uci.edu.

*Abbreviations:* FTIR, Fourier transform infrared spectroscopy; DPPC, dipalmitoylphosphatidylcholine; TFA, trifluoroacetic acid; TFE, trifluoroethanol; EYL, egg yolk lecithin; PG, phosphatidyl glycerol; Tanaka lipids, DPPC/unsat. PG/palmitic acid (66:22:9, wt%); PBS, phosphate-buffered saline; ATR, attenuated total reflectance; NS, nitroxide stearate; SP-B, surfactant protein B; SP-$B_{1-25}$, N-terminal domain of SP-B, residues 1–25; SP-$B^{*}_{1-25}$, amino spin-labeled N-terminal domain of SP-B, residues 1–25; SP-$B_{1-9}$, truncated N-terminal segment of SP-B, residues 1–9; SP-$B_{8-25}$, truncated N-terminal segment of SP-B, residues 8–25; SP-$B_{15-25}$, truncated N-terminal segment of SP-B, residues 1–9; SP-$B_{15-25}$, truncated N-terminal segment of SP-B, residues 15–25; $a'_N$, isotropic hyperfine coupling constant; $S$, polarity-corrected order parameter; ESR, electron spin resonance; $[\theta]_{MRE}$, mean residue ellipticity (deg cm$^2$ dmol$^{-1}$).

Surfactant protein B is a small, lipid-associating protein found in mammalian lung surfactant (Possmayer, 1988). The protein is encoded on chromosome two and synthesized in type II pneumocytes. The mature protein is very hydrophobic and partitions into the chloroform phase with surfactant lipids when isolated from lung lavage using the Folch et al. (1957) extraction procedure. Plasma desorption mass spectral analysis of native SP-B indicates that the protein has no posttranslational modifications other than disulfide bond formation (Curstedt et al., 1990). The dominant molecular species of SP-B is a disulfide-linked homodimer, although variable amounts of monomeric SP-B are also observed in samples isolated from lung surfactant. Each monomeric unit has disulfide links at the mid-sequence and N-terminal and C-terminal sections, suggesting the main chain may assume a hairpin-like format. The N-terminal amphipathic domain has a unique primary sequence, with a short hydrophobic multiple proline segment that includes the N-terminal phenylalanine residue and is adjacent to a theoretically predicted amphipathic helical segment.

A unique primary structure for SP-B suggests specific protein domain function. One major role of SP-B in the lung is the interaction with surfactant lipids that maintains a monolayer film at the dynamically changing alveolar air interface required for gas exchange. The N-terminal sequence of SP-B ($SP\text{-}B_{1\text{-}25}$, residues 1–25; Fig. 1) has been shown to have very specific interactions with amphipathic lipids. The positively charged amino terminus of SP-B increases the collapse pressure of surfactant lipid monolayers containing palmitic acid, suggesting that this cationic peptide interacts with specific anionic lipids to remove the driving force for squeeze-out of the lipid from the surface film (Longo et al., 1993; Lipp et al., 1996). Another indication of specific interaction of SP-B with lipids is insertion of the protein into monolayers at varying surface pressures (Oosterlaken-Dijksterhuis et al., 1991). The critical insertion pressure, an index of the degree of peptide association with lipid films and membrane systems, is very high for the amino-terminal peptide of SP-B in contrast to the C-terminal domain of the protein (Bruni et al., 1991; Fan et al., 1991). The N-terminal domain of SP-B has also been shown to mediate lipid-vesicle mixing (Longmuir et al., 1992), as does the native SP-B (Oosterlaken-Dijksterhuis et al., 1992).

Both theoretical and experimental studies have been performed to assess the secondary and tertiary conformations of SP-B. Theoretical analysis of the primary sequence of SP-B, using the hydrophobic moment algorithm and Chou–Fasman secondary structure predictions, suggests several amphipathic

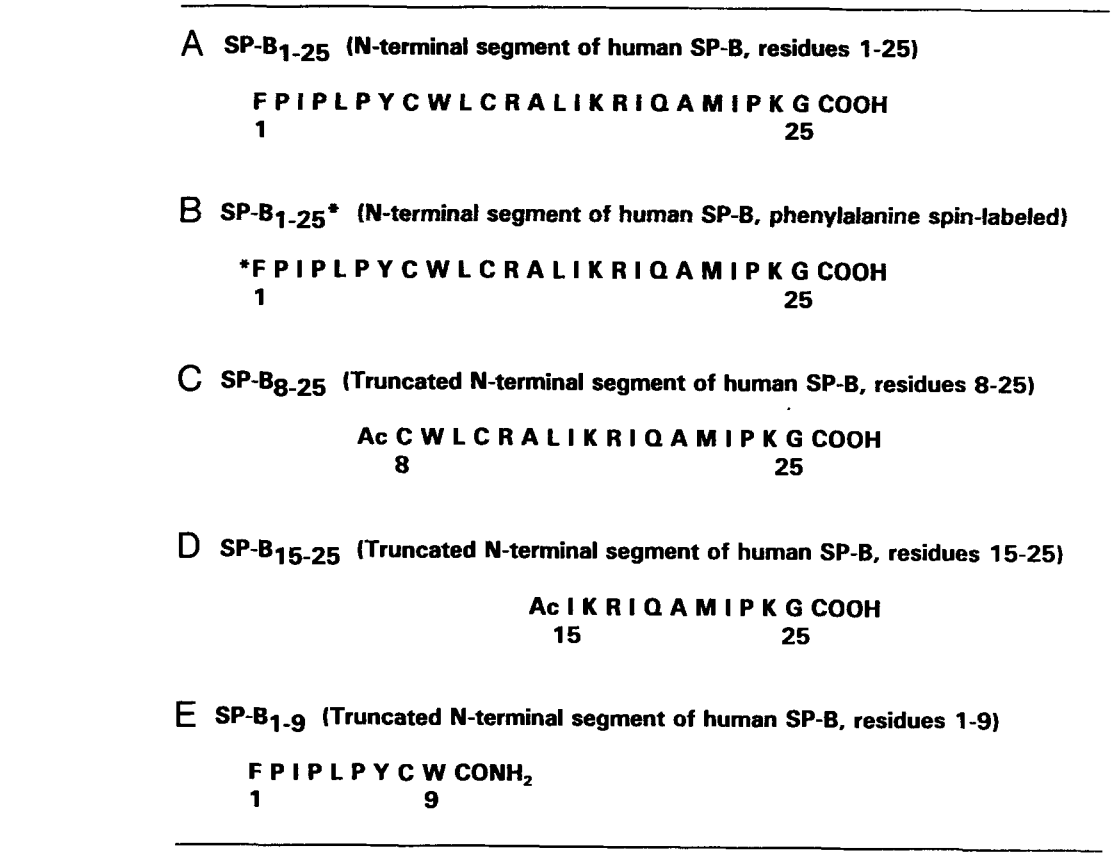


**Fig. 1.** Amino acid sequences of peptides derived from the N-terminal segment of human SP-B, residues 1–25. Residues are numbered from the N-terminal phenylalanine; one-letter codes for amino acids are used. Ac indicates N-acetylation of the peptide, and $CONH_2$ represents carboxyamidation of the C-terminal residue. **A:** $SP\text{-}B_{1\text{-}25}$, the N-terminal segment of SP-B, residues 1–25. **B:** $SP\text{-}B^{*}_{1\text{-}25}$, the N-terminal segment of SP-B, residues 1–25, spin-labeled at the amino-terminal phenylalanine (F*) with succinimidyl 2,2,5,5-tetramethyl 3-pyroline. **C:** $SP\text{-}B_{8\text{-}25}$, amphipathic helical domain of the N-terminal segment of SP-B, residues 8–25. **D:** $SP\text{-}B_{15\text{-}25}$, amphipathic helical domain of the N-terminal segment of SP-B, residues 15–25. **E:** $SP\text{-}B_{1\text{-}9}$, insertion domain of the N-terminal segment of SP-B, residues 1–9.

helical segments near the N-terminus and C-terminus of the 78-residue molecule (Waring et al., 1989; Takahashi et al., 1990; Bruni et al., 1991). CD, FTIR, and Raman spectroscopy of native SP-B and selected amphipathic segments indicates a dominant helical conformation in structure-promoting solvents, such as TFE:water, surfactant lipid dispersions, oriented lipid films, and detergent micelle dispersions (Bruni et al., 1991; Fan et al., 1991; Vincent et al., 1991; Longo et al., 1992; Oosterlaken-Dijksterhuis et al., 1992; Vandenbussche et al., 1992; Pérez-Gil et al., 1993). Oriented CD measurements and polarized FTIR determinations of the native protein in surfactant lipid films further indicate that the protein helical axis is oriented approximately parallel to the surface of the film (Oosterlaken-Dijksterhuis et al., 1991; Vandenbussche et al., 1992).

Other physical experiments on the topography of SP-B in surfactant lipid dispersions and membrane-mimic environments have suggested that the protein lies near the polar headgroup. For example, studies with fluorescent lipids, NMR measurements of deuterated surfactant lipids, and determinations of lipid ordering with Raman spectroscopy indicate that addition of native SP-B, or synthetic peptide mimics, changes the molecular order of the lipid near the polar interface (Baatz et al., 1990; Vincent et al., 1991, 1993; Wiedman, 1991; Morrow et al., 1993). An early ESR study of synthetic surfactant lipid dispersions incorporated with spin-labeled phospholipid showed that addition of native SP-B, or synthetic peptides based on human SP-B, increases the molecular ordering of the lipid dispersion near the five-carbon position of the phospholipid acyl chains (Waring et al., 1989). A more recent examination (Pérez-Gil et al., 1995) of lipids labeled with phospholipid spin probes not only confirmed that SP-B decreased the motional flexibility in the lipid headgroup, but also indicated that this motional restriction extended more or less uniformly throughout the length of the lipid chains. Pérez-Gil et al. (1995) suggested that these effects could be due to direct SP-B interactions with either the lipid headgroup region or fatty acyl chains embedded in deeper regions of the bilayer. Clearly, physical studies that examine solely protein perturbations on lipid flexibility cannot unequivocally assign the location of SP-B in lipid bilayers or monolayers.

Despite considerable information on the overall conformation of SP-B in lipid dispersions, and also on the interactions of this protein with lipid dispersions, much less is known about the residue-specific topography of SP-B in surfactant lipids and structure-promoting environments such as detergent micelles. Greater details on the residue-specific interactions of SP-B domains may provide a better understanding of the structure-function correlates of this protein. In the present study, we describe the interaction of several key amino acid residues of the N-terminal SP-$B_{1-25}$ peptide in various structure-promoting environments. Results from these experiments have led to a more precise model for SP-$B_{1-25}$ interacting with surfactant lipid dispersions.

## Results

### *Conformation and helical axis orientation of SP-$B_{1-25}$ in structure-promoting environments*

Measurements of SP-$B_{1-25}$ were made in several simple solvents that were found to optimize the secondary conformation of the N-terminal segment. For SP-$B_{1-25}$ suspended in a series of solvents and interfacial-mimic systems, typical FTIR spectra of the amide-I band are shown in Figure 2. Curve fitting of the spectra (Fig. 3; Table 1) indicates that SP-$B_{1-25}$ has a dominant helical component (centered at 1,658 $cm^{-1}$) in methanol and other structure-promoting environments. Other assignments of the secondary structure of SP-$B_{1-25}$ used the criteria of Susi and Byler (1986), and indicated disordered (random) structures about 1,645 $cm^{-1}$, a beta sheet component at 1,630 $cm^{-1}$, and possible beta turns from 1,660 to 1,682 $cm^{-1}$. The relative proportions of the secondary conformation components were very similar for each of the structure-promoting environments, which included methanol, SDS micelles, EYL multilammelar vesicles, and synthetic surfactant lipid dispersions (i.e., Tanaka lipids) (Table 1).

Smaller peptides based on SP-$B_{1-25}$ were also studied in methanol to localize the above structural features. The C-terminal segment of SP-$B_{1-25}$ comprising residues 15–25 (i.e., SP-$B_{15-25}$) had a distinctly different FTIR-amide I spectrum (Fig. 4C) than that of the full-length 25-residue peptide (Fig. 3). The major FTIR peak for SP-$B_{15-25}$ was at 1,637 $cm^{-1}$, with less intense contributions at 1,645 $cm^{-1}$, 1,658 $cm^{-1}$, and 1,674 $cm^{-1}$. Complementary CD spectra (Fig. 5B) of the peptide in methanol show dichroic minima at 222 and 205 nm, typical of a helix-like structure with ≈36.7% helical conformation based on the 222-nm dichroic minimum. These FTIR and CD observations suggest that SP-$B_{15-25}$ may assume structures characteristic of Type III $\beta$ turns or $3_{10}$ helix, as well as $\alpha$ helix and disordered conformations (Miick et al., 1992; Fiori & Millhauser, 1995). When the C-terminal segment is extended to include residues 8–25 (i.e., SP-$B_{8-25}$), the FTIR-amide I spectrum (Fig. 4B) indicates a major $\alpha$ helical component centered at 1,658 $cm^{-1}$.

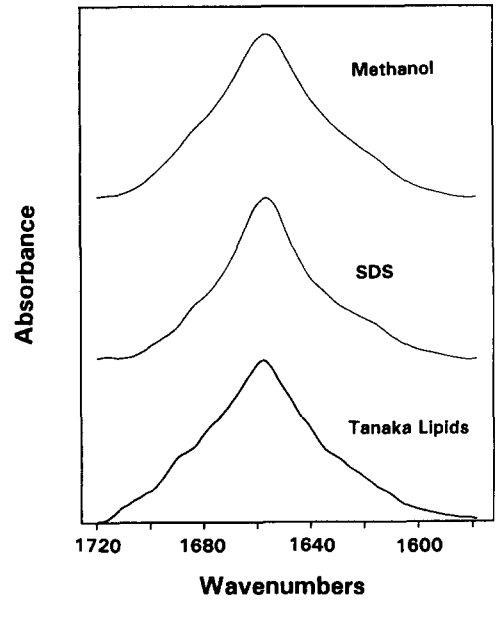


**Fig. 2.** Fourier transform infrared (FTIR) spectra of the amide I band of SP-$B_{1-25}$, in such structure-promoting environments as methanol, SDS, and Tanaka lipids. The peptide solution was made in methanol at a concentration of 170 $\mu$M. The respective lipid to peptide ratios for the SDS and Tanaka lipid samples were 300:1 and 150:1. Tanaka lipids are defined in Materials and methods. Spectra have been normalized for comparison.

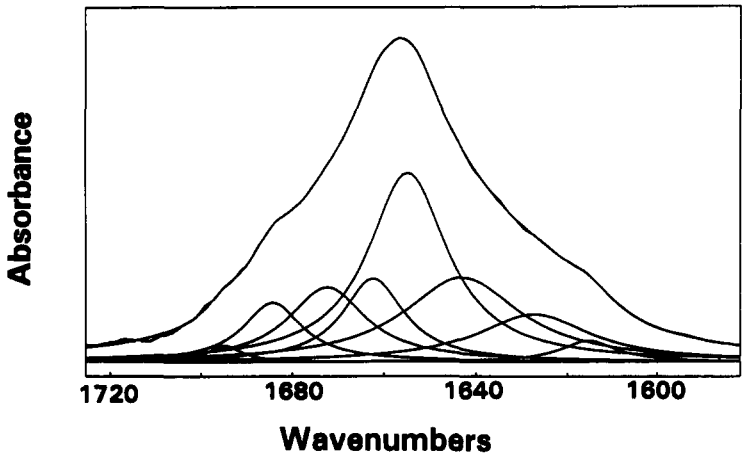


**Fig. 3.** Representative FTIR spectra and curve fitting of the amide I band of SP-$B_{1-25}$ in methanol. Top curve is the experimental FTIR spectrum of the amide I band. Frequency limits for different secondary structures were as follows: $\alpha$ helix, 1,662–1,645 $cm^{-1}$; beta sheet, 1,637–1,613 $cm^{-1}$ and 1,689–1,682 $cm^{-1}$; beta turns, 1,682–1,662 $cm^{-1}$; and disordered structure (random), 1,645–1,637 $cm^{-1}$. The % contributions for each component are shown in Table 1. Overlapping the experimental spectrum is the predicted spectrum, summing the above components. SP-$B_{1-25}$ concentration was 170 $\mu$M.

Fourier self deconvolution and curve-fitting confirmed that the predominant conformation for SP-$B_{8-25}$ in methanol was helical, but also indicated $\beta$-sheet and $\beta$-turn contributions (Table 2). CD analysis of SP-$B_{8-25}$ in methanol showed typical $\alpha$ helical-like spectra (Fig. 5C) with a well-defined double minima at 222 and 208 nm and $\approx$35.4% helix. In this context, it should be noted that the corresponding CD spectrum of the full-length SP-$B_{1-25}$ in methanol (Fig. 5A) also indicated a substantial helical component (46.6% helix), with a well-defined double minimum at 222 and 208 nm. Given the above FTIR and CD results with the full-length and truncated SP-$B_{1-25}$ peptides, it is likely that the segment spanning residues 8–25 assumes the dominant helical conformation in the full-length SP-$B_{1-25}$ peptide.

CD and FTIR studies were also performed with the SP-$B_{1-9}$ peptide, which includes the hydrophobic, proline-rich N-terminus and predicted tetra-peptide B-turn element (Fig. 1). FTIR spectra of SP-$B_{1-9}$ in methanol showed major components at 1,662, 1,656, 1,641, and 1,633 $cm^{-1}$, suggesting populations of $\beta$-turn and helical conformers (Hollosi et al., 1994). Fourier self deconvolution and curve fitting indicated that $\beta$-turn structures were the principal conformation for SP-$B_{1-9}$ in methanol, although significant contributions were also found for $\beta$-sheet and helical conformations (Table 2). CD measurements of SP-$B_{1-9}$, suspended in methanol (Fig. 5D), also confirm turn and helical propensities of the N-terminal segment, and indicate possible type I $\beta$-turn character (Perczel et al., 1993). Our finding that SP-$B_{1-9}$ assumes multiple conformations in methanol may be because the many proline residues confer a dynamic quality to the sequence, thereby fraying the conformation of this short N-terminal segment. In light of our FTIR results indicating a significant $\beta$-turn conformation for SP-$B_{1-25}$ suspended in methanol and that the principal conformation for SP-$B_{1-9}$ in this solvent is $\beta$-turn, residues 1–9 probably assumes $\beta$-turn in the full-length peptide.

Polarized FTIR measurements were also performed on the SP-$B_{1-25}$ peptide in self films spread from solvents onto germanium ATR substrates, and in multilayer films of SDS, EYL, and synthetic surfactant lipids (i.e., DPPC:PG and Tanaka lipids) using the ATR technique (Goormaghtigh et al., 1990). When a portion of the SP-$B_{1-25}$ peptide assumes a helical conformation, this allows the determination of the angle ($\theta$) of the heli-

**Table 1.** *Helical axis orientation and proportions of secondary structure for SP-$B_{1-25}$ in solvents and lipid dispersion films, as estimated from Fourier self-deconvolution of the FTIR spectra of the peptide amide I band*

| | % Conformation[a] | | | | Orientation | |
|---|---|---|---|---|---|---|
| System | $\alpha$-Helix | $\beta$-Sheet | $\beta$-Turn | Disordered | $R_{ATR}$[b] | Angle[c] |
| Methanol | 37.3 | 12.6 | 27.4 | 22.7 | 1.22[d] | 40 degrees |
| SDS | 42.5 | 14.4 | 26.4 | 16.7 | 1.31 | 50 degrees |
| EYL | 36.2 | 14.7 | 31.8 | 17.3 | 1.28 | 45 degrees |
| DPPC/PG | 40.6 | 14.2 | 27.7 | 17.5 | 1.29 | 45 degrees |
| Tanaka lipids | 39.0 | 17.2 | 29.8 | 14.0 | 1.29 | 45 degrees |

[a] Data are the means of four separate determinations and have an SE $\pm$ 5% or better.

[b] $R_{ATR}$ is the dichroic ratio $A_{90}/A_0$, where $A_{90}$ is the polarized absorbance measurement perpendicular to the ATR plate, and $A_0$ is the polarized absorbance measurement parallel to the ATR plate. Angles estimated from parametric plot of $R_{ATR}$ as a function of the order parameter according to Brauner et al. (1987).

[c] This measurement represents the angle with respect to the plane of the lipid-bulk aqueous interface, and is the mean of four separate determinations with an SE of $\pm$ 3 degrees.

[d] SP-$B_{1-25}$ sample (10–100 $\mu$g peptide) dried on to ATR plate from a methanol solution.

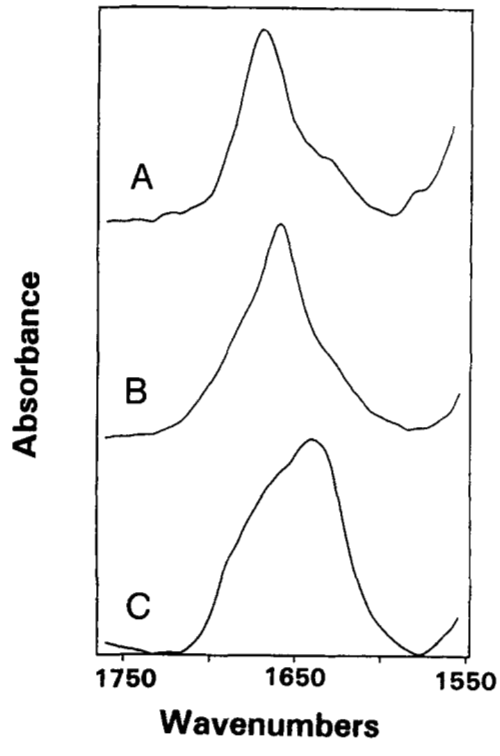


**Fig. 4.** Amide I region of the FTIR spectrum of truncated peptides of the SP-B N-terminal segment in methanol. **A:** SP-$B_{1-9}$, at a concentration of 440 $\mu$M. **B:** SP-$B_{8-25}$, at a concentration of 238 $\mu$M. **C:** SP-$B_{15-25}$, at a concentration of 403 $\mu$M.

cal axis with respect to the surface of the germanium substrate (Table 1). Because the conformation of peptides and proteins is essentially unaltered by drying the sample on an appropriate ATR crystal from a structure-promoting solvent system (Goormaghtigh et al., 1990), measurements were made on the self-films of peptide dried from methanol or hexafluoroisopropanol. The SP-$B_{1-25}$ helical component in self-films exhibited an oblique angle ($\theta$) to the surface of the polar ATR crystal in the absence of lipid (Table 1), confirming the overall amphipathic character of the major helical component on the peptide. For SP-$B_{1-25}$ incorporated into detergent SDS, the angle ($\theta$) for the peptide helical axis significantly increased (Table 1), indicating an enhanced angle of insertion with respect to the surface of the germanium-SDS film; on the other hand, the SDS acyl chains were oriented near to the normal ($R_{ATR} = 1.21$) of the crystal surface. When SP-$B_{1-25}$ was dispersed into EYL or synthetic surfactant lipids (DPPC:PG and Tanaka lipids), the $\theta$ for the peptide helical axis with respect to the germanium-lipid film was intermediate to that observed with methanol and SDS (Table 1). Contrarily, the acyl chains of the lipid-peptide films were oriented close to normal (EYL, $R_{ATR} = 1.54$; Tanaka lipids, $R_{ATR} = 1.06$) with respect to the surface of the germanium substrate. The truncated surfactant peptide SP-$B_{8-25}$ had an $R_{ATR}$ of 1.23 and a $\theta$ of 40° for peptide in EYL and Tanaka lipid films, suggesting that deletion of N-terminal residues 1-7 altered the mean orientation of the helical component in these lipid environments.

**Table 2.** *Proportions of secondary structure for SP-$B_{1-25}$ and truncated SP-$B_{1-25}$ peptides in the structure-promoting solvent methanol, as estimated from Fourier self-deconvolution of the FTIR spectra of the peptide amide I band*

| | % Conformation for peptides in methanol[a] | | | |
|---|---|---|---|---|
| Peptide | Helix | $\beta$-Sheet | $\beta$-Turn | Disordered |
| SP-$B_{1-9}$ | 16.3[b] | 26.3 | 38.4 | 19.0 |
| SP-$B_{8-25}$ | 44.0[b] | 8.8 | 34.9 | 12.3 |
| SP-$B_{1-25}$ | 37.3[c] | 12.6 | 27.4 | 22.7 |

[a] Data are the mean of four separate determinations and have an SE ± 5% or better. Peptide samples (10–100 $\mu$g) were dried on to the ATR plate from methanol solution.

[b] Percent helix includes $3_{10}$ (1,638 $cm^{-1}$) and $\alpha$-helix (1,656 $cm^{-1}$) spectral contributions.

[c] Percent helix includes the $\alpha$-helix (1,656 $cm^{-1}$) spectral contribution.

### *ESR studies with the spin-labeled N-terminal SP-$B^*_{1-25}$ peptide*

Initial ESR studies were performed on the spin-labeled N-terminal SP-B peptide [SP-$B^*_{1-25}$; Fig. 1] suspended in either methanol (100%) or PBS. Figure 6A shows that, at a peptide concentration of 273 $\mu$M in methanol, SP-$B^*_{1-25}$ exhibits nearly isotropic motion at 39 °C with minimal probe-probe interactions due to peptide aggregation (Curtain et al., 1987). Accordingly, this spectrum may be analyzed for probe mobility and polarity by calculating a rotational correlation time ($\tau_R = 1.55 \times 10^{-10}$ sec) and an isotropic hyperfine coupling constant ($a'_N = 15.34$ gauss). The low $\tau_R$ confirms that the covalently attached reporter group is rapidly tumbling in methanol, whereas the $a'_N$ value is consistent with SP-$B^*_{1-25}$ sampling a relatively hydrophobic environment (Jost & Griffith, 1978).

The ESR spectrum for 14.3 $\mu$M SP-$B^*_{1-25}$ suspended in PBS (Fig. 6B) is very different than that obtained for spin-labeled peptide in methanol (Fig. 6A). Figure 6B shows that the spin-labeled peptide samples two distinct environments in aqueous solution. The first component is spectral broadened, indicating that SP-$B^*_{1-25}$ here resides in an environment that is motionally restricted. Besides restricted flexibility, this broadened spectral component may be partially a consequence of nitroxide radical interactions (i.e., dipolar broadening and spin-spin exchange) between aggregated SP-$B^*_{1-25}$ molecules (Sauerheber et al., 1977; Curtain et al., 1987). The second component shows sharp lines (see arrows in Fig. 6B), denoting probe covalently attached to SP-$B^*_{1-25}$ rapidly tumbling in a fluid environment. This freely mobile SP-$B^*_{1-25}$ resides in a relatively aqueous environment, as indicated by the high $a'_N$ (=16.42 G; Table 3). One interpretation of the freely mobile component is that it is due to monomeric SP-$B^*_{1-25}$ rapidly tumbling in PBS. Alternatively, this component may be due to probe, which is part of aggregated SP-$B^*_{1-25}$, but with the nitroxide reporter extending into the aqueous medium, where it is unaggregated and mobile. The well-resolved sharp-line and broadened components in Figure 6B indicate that exchange of SP-$B^*_{1-25}$ between the two environments occurs slowly on the ESR time scale (i.e., $> 10^{-8}$ sec). Estimates from double integration of the component ESR spectra

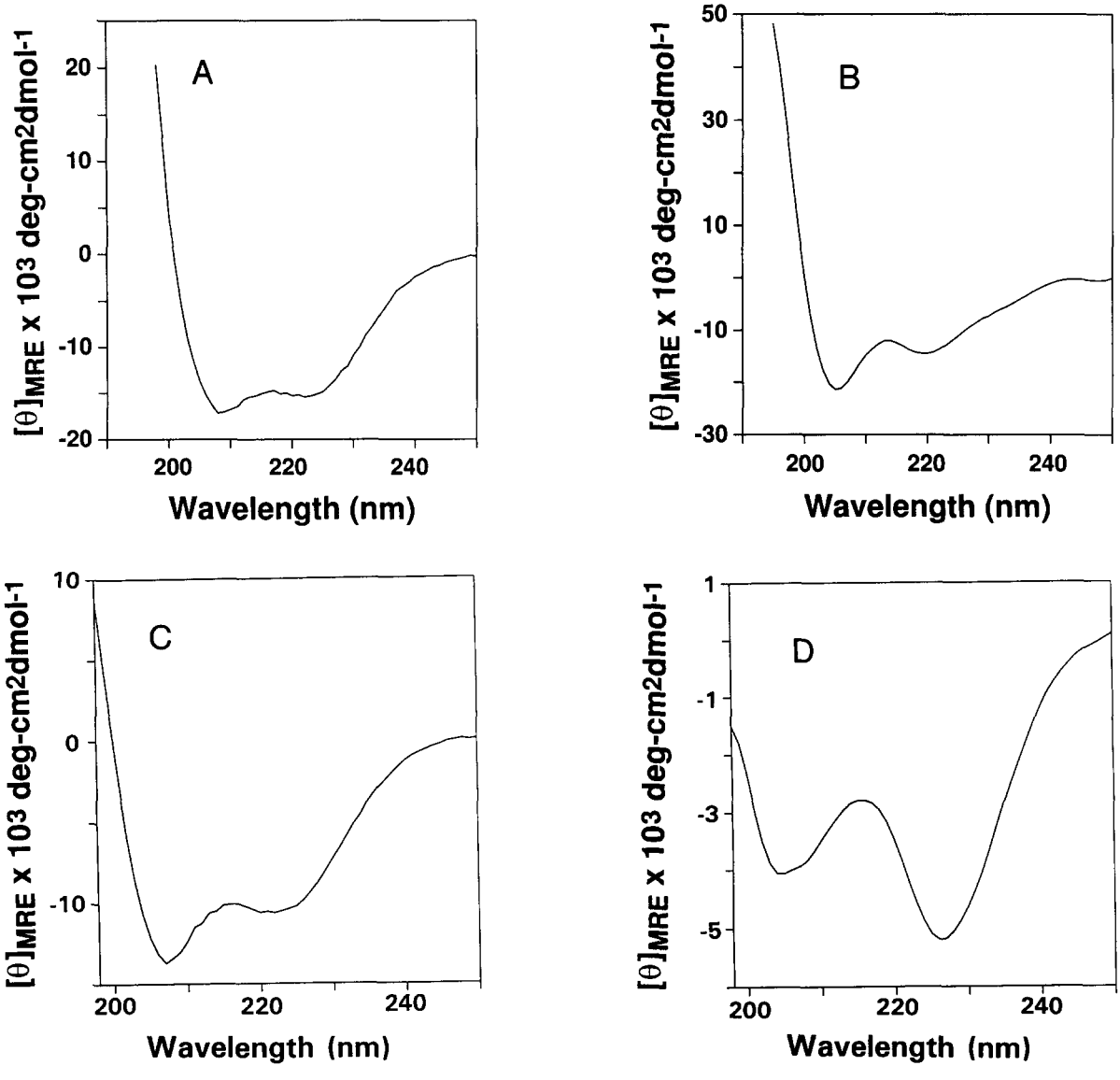


**Fig. 5.** CD spectra of the full-length and truncated peptides, based on the SP-B N-terminal segment (residues 1-25) in methanol and showing the mean residue ellipticities [$(\theta) \times 10^{-3}$ (deg cm$^2$ dmol$^{-1}$)]. **A:** SP-$B_{1-25}$. **B:** SP-$B_{15-25}$. **C:** SP-$B_{8-25}$. **D:** SP-$B_{1-9}$. Peptide concentrations were 20 $\mu$M. The optical pathlength was 1 mm and the temperature was 38 °C. Spectra represent the average of 8 scans.

in Figure 6B indicate that the predominant species (>97%) of SP-$B^*_{1-25}$ in PBS is broadened (Curtain et al., 1987).

The respective environments for SP-$B^*_{1-25}$ in PBS may be further probed using the paramagnetic broadening agent chromium oxalate (Altenbach & Hubbell, 1988). Chromium oxalate (50 mM) obliterates the sharp "liquid-line" component (Fig. 6C); the hydrophilic, broadening agent achieves this through direct collisions with the SP-$B^*_{1-25}$ reporter group in an aqueous environment, which shorten the electron relaxation time. This confirms our initial assignment that the sharp-line component in Figure 6B was due to the reporter of SP-$B^*_{1-25}$ residing in aqueous medium. Contrarily, chromium oxalate only partially reduces the spectral-broadened component for SP-$B^*_{1-25}$ in PBS (Fig. 6C), suggesting that aggregated SP-$B^*_{1-25}$ in Figure 6B consists of chromium oxalate-sensitive and -insensitive components. It should be noted that the SP-$B^*_{1-25}$ uptake in PBS (Fig. 6B) is exceedingly low. The % probe uptake for spin-labeled peptide added at 109 $\mu$M SP-$B^*_{1-25}$ in PBS "wt" (Fig. 6B; see Materials and methods) was only 13%, consistent with the formation of peptide aggregates having limited solubility. Consequently, the low signal/noise for the spectrum of SP-$B^*_{1-25}$ in PBS (Fig. 6B,C) precludes a more rigorous motional and broadening analysis.

It is of interest to further examine the $a'_N$ values for SP-$B^*_{1-25}$ residing in either methanol (100%) (Fig. 6A) or the sharp-line component in PBS (Fig. 6B). The $a'_N$ for SP-$B^*_{1-25}$ in methanol (= 15.34 G) is similar to that of the free spin label (i.e., succinimidyl 2,2,5,5-tetramethyl-3-pyrroline-1-oxyl-3-carboxylate) in methanol (= 15.21 G). Furthermore, the $a'_N$ for the sharp-line component of SP-$B^*_{1-25}$ in PBS (= 16.42 G) is comparable to

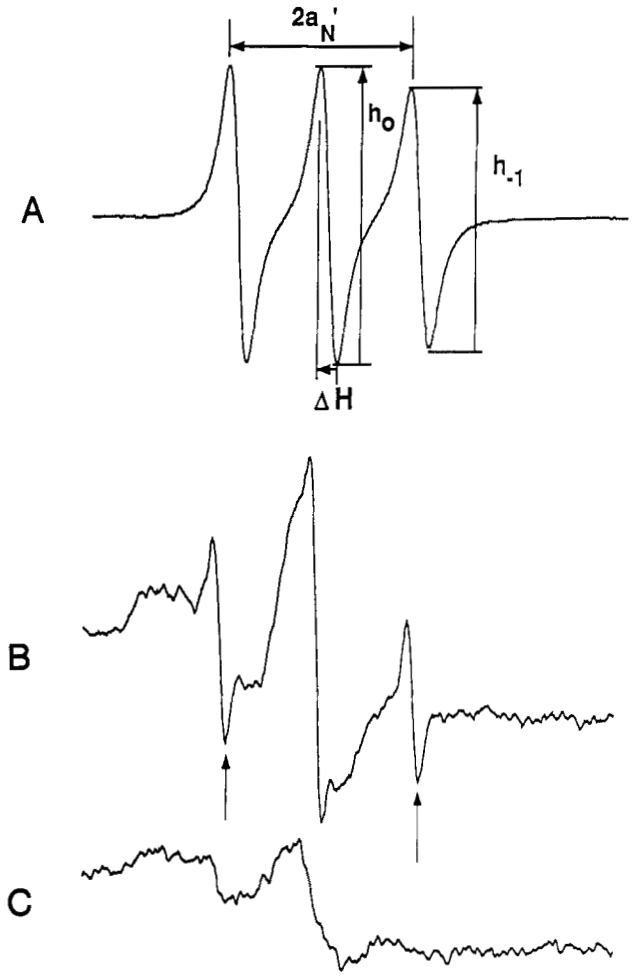


**Fig. 6.** ESR spectra of the amino-spin-labeled peptide (i.e., SP-$B^*_{1-25}$) in (**A**) methanol, (**B**) PBS, and (**C**) PBS and chromium oxalate at 39 °C. **A:** SP-$B^*_{1-25}$ residues in a single environment in methanol (100%), and exhibits rapid tumbling about all three molecular axes. The peak heights, $h_{-1}$ and $h_o$, as well as the peak-to-peak distance ($\Delta H_o$) of the central band, were measured as shown. The $\tau_R$ was equal to $1.55 \times 10^{-10}$ s (Table 3), as determined from Equation 1. The isotropic hyperfine coupling constant ($a'_N$ = 15.34 G) was also measured (Knowles et al., 1976). **B:** SP-$B^*_{1-25}$ samples two distinct environments in PBS. A motionally restricted (broadened) component indicates aggregated peptide, whereas a sharp three-line component (see arrows) indicates probe attached to SP-$B^*_{1-25}$ tumbling rapidly in an aqueous environment. The *x*-axis distance between the two arrows represents the $2a'_N$ value (=32.84 G) for probe attached to SP-$B^*_{1-25}$ undergoing nearly isotropic motion in an aqueous environment. **C:** Addition of 50 mM-chromium oxalate to SP-$B^*_{1-25}$ in PBS eliminates the aqueous, "liquid-line" SP-$B^*_{1-25}$, without influencing the spectral component arising from aggregated spin-labeled peptide. The respective $\mu$M/L concentrations for SP-$B^*_{1-25}$ in methanol and PBS were 273 and 14.3. Spectra were recorded with a scan time of 8 min and a time-constant of 1 s. *x* axis, end-to-end of spectra is equal to 90 Gauss. Probe concentrations were determined from double-integration of the ESR spectra as described in the text.

that noted for the free spin label in PBS (= 16.26 G). The above findings indicate that covalent attachment of SP-$B_{1-25}$ to the spin label does not affect the polarity of the probe environment in these two solvents. These results also suggest that the nitroxide group does not participate in the backbone conformation of SP-$B^*_{1-25}$.

Additional studies were performed to examine the interactions of SP-$B^*_{1-25}$ with SDS at 39 °C. At the detergent concentration (20 mM) used here, SDS is micellar and, thus, presents a macromolecular assembly that resembles an anionic membrane. Figure 7A shows the ESR spectrum of SDS with SP-$B^*_{1-25}$ at a peptide/lipid ratio of 1/557. The spectrum indicates that SP-$B^*_{1-25}$ binds to micellar SDS, and exhibits motion slower than that noted for SP-$B^*_{1-25}$ in methanol (Fig. 6A), but much faster than that seen for aggregated peptide in PBS (Fig. 6B,C). The $\tau_R$ (= $28.6 \times 10^{-10}$ s) in Table 3 confirms that SP-$B^*_{1-25}$ is only "weakly immobilized" when bound to SDS. At the peptide/lipid ratio used here, Figure 7A indicates minimal aggregation for the spin-labeled peptide in SDS micelles (Sauerheber et al., 1977; Curtain et al., 1987), particularly when compared with the aggregated spectrum of SP-$B^*_{1-25}$ in PBS (Fig. 6B).

ESR spectra further indicate that SP-$B^*_{1-25}$ also binds to EYL liposomes (Fig. 7D), a mixture of DPPC and unsaturated PG

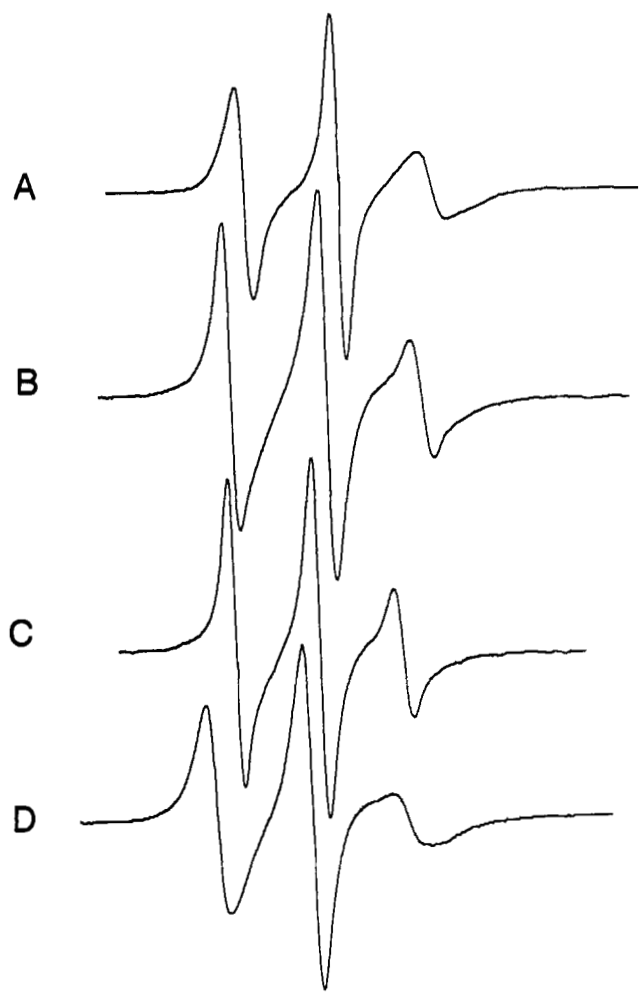


**Fig. 7.** ESR spectra of the amino-spin-labeled peptide (i.e., SP-$B^*_{1-25}$) in various lipids at 39 °C. **A:** SP-$B^*_{1-25}$ and SDS (20 mM) in PBS at a peptide/lipid ratio of 1/557. **B:** SP-$B^*_{1-25}$ and DPPC/PG in PBS at a peptide/lipid ratio of 1/2175. **C:** SP-$B^*_{1-25}$ and Tanaka lipids in PBS at a peptide/lipid ratio of 1/2720. **D:** SP-$B_{1-25}$ in EYL at a peptide/lipid ratio of 1/1818. *x* axis, end-to-end of spectra is equal to 90 Gauss. Probe concentrations were determined from double-integration of the ESR spectra as described in the text.

**Table 3.** *ESR spectral parameters for 5-NS with EYL and SP-$B^*_{1-25}$ with methanol, EYL, SDS, and surfactant lipids at 39 °C*[a]

| Solvent/lipid | Probe concentration[b] | $\tau_R$ (sec)[c] × $10^{10}$ | $a'_N$ (G) | $S$[d] |
|---|---|---|---|---|
| Methanol (100%) | 273 μM SP-$B^*_{1-25}$ | 1.55 (0.06) | 15.34 (0.06)[e] | – |
| PBS ("liquid-line") | 14.3 μM SP-$B^*_{1-25}$ | – | 16.42 (0.16)[e] | – |
| SDS (20 mM) | 1 SP-$B^*_{1-25}$/557 lipid | 28.6 (3.4) | 15.77 (0.05)[e] | – |
| EYL (48 mg/mL) | 1 SP-$B^*_{1-25}$/1818 lipid | 33.8 (1.2) | 16.10 (0.01)[e] | – |
| EYL (48 mg/mL) | 1 5-NS/1401 lipid | – | 14.97 (0.06)[f] | 0.397 (0.003) |
| DPPC/PG (unsat.) | 1 SP-$B^*_{1-25}$/2175 lipid | 17.7 (1.2) | 16.05 (0.03)[e] | – |
| Tanaka lipids | 1 SP-$B^*_{1-25}$/2720 lipid | 13.4 (1.0) | 16.13 (0.04)[e] | – |

[a] Number of measurements = 4 for $\tau_R$, $a'_N$, and $S$ determinations. Values are means, with 1 SD in parentheses.
[b] Probe concentration was expressed either in μM (methanol or PBS), or probe/lipid ratio, determined from double-integration of ESR spectra (see Materials and methods). Spin-labeled N-terminal SP-B peptide (SP-$B^*_{1-25}$) is defined in Figure 1.
[c] $\tau_R$, the rotational correlation time, was calculated from Equation 2.
[d] $S$, the polarity-corrected order parameter, was calculated from Equation 3.
[e] $a'_N$, the isotropic hyperfine coupling constant in Gauss, was calculated as shown in Figure 6A.
[f] $a'_N$, the isotropic hyperfine coupling constant in Gauss was calculated from $\frac{1}{3}\cdot(T_\parallel + 2T_\perp)$ G, where $T_\parallel$ and $T_\perp$ were measured as in Figure 8C and D.

(Fig. 7B), and Tanaka lipids (Fig. 7C). Similar to that noted for SP-$B^*_{1-25}$-labeled SDS, the spin-labeled, N-terminal peptide of SP-B is relatively "weakly immobilized" for each of these lipids at 39 °C. However, the $\tau_R$s in Table 3 indicated that there were variations in the motion of SP-$B^*_{1-25}$ in each of the lipids, with the following order for reporter group mobility: Tanaka lipids ~ DPPC + PG > SDS ~ EYL. Similar to that noted for SP-$B^*_{1-25}$ with SDS (Fig. 7A), there is minimal indication of probe-probe interactions or spin-labeled peptide aggregation in the ESR spectra (Fig. 7B,C,D) for any of these lipids.

It is important to assess the vertical degree of penetration into the lipid (or micellar SDS) of the N-terminus reporter group for SP-$B^*_{1-25}$. One approach is to examine the ESR spectral broadening observed with the addition of chromium oxalate to SP-$B^*_{1-25}$ labeled lipids. With SP-$B^*_{1-25}$-labeled EYL liposomes, chromium oxalate (50 mM) had no effect on the ESR spectrum (Fig. 8A,B). This indicates that the nitroxide reporter group must be embedded in the lipid bilayer to prevent direct contact with the negatively charged chromium oxalate. Similar experiments indicated no spectral broadening effects of chromium oxalate on SP-$B^*_{1-25}$-labeled SDS, DPPC + PG, or Tanaka lipids (data not shown). For each of these lipids, the reporter group for SP-$B^*_{1-25}$ must sufficiently penetrate into the lipid bilayer (or micelle) to avoid chromium oxalate.

Another method for evaluating penetration into the bilayer (or micelle) is to measure the $a'_N$ of the SP-$B^*_{1-25}$ labeled lipids. Table 3 shows relatively high $a'_N$ values for SP-$B^*_{1-25}$ in each lipid (i.e., $15.77 < a'_N < 16.13$ G); such high $a'_N$ values preclude deep penetration of the N-terminal group into the hydrocarbon interior, but instead argue that the reporter group of SP-$B^*_{1-25}$ resides near the polar headgroup region (Jost & Griffith, 1978). This is illustrated most clearly with SP-$B^*_{1-25}$-labeled EYL liposomes. Seelig and Hasselbach (1971) previously have shown the existence of a vertical flexibility and polarity gradient in EYL liposomes. Their approach used a suite of stearic-acid (NS) spin probes as a reference "dipstick," indicating a relatively rigid, polar surface and a fluid, hydrophobic interior. Comparison of the $a'_N$ values for NS-labeled EYL liposomes with that obtained for SP-$B^*_{1-25}$ (Fig. 9) indicates that the reporter group of the spin-labeled surfactant peptide must lie closer to the polar headgroup than the 5-C position of the 5-NS probe. Interestingly, addition of chromium oxalate to 5-NS labeled EYL did not affect the ESR spectrum (Fig. 8C,D), similar to that noted for SP-$B^*_{1-25}$ (Fig. 8A,B).

### *Endogenous tryptophan fluorescence of SP-$B_{1-25}$ in structure-promoting environments*

Additional residue-specific information on the incorporation of SP-$B_{1-25}$ into various structure-promoting environments may be obtained by measuring the endogenous fluorescence of the Trp-9. Because tryptophan emission is hydration dependent, the insertion of this aromatic residue into more hydrophobic environments (e.g., lipids) from a more polar, aqueous solvent may be monitored by a shift in the fluorescence maximum to lower wavelengths. When SP-$B_{1-25}$ is suspended in PBS, there was a small "blue" shift to lower wavelengths (Table 4); this suggests that Trp-9 samples a slightly less polar environment for SP-$B_{1-25}$ in PBS than when this peptide is in water. The "blue" shift in the fluorescence maximum for SP-$B_{1-25}$ is most likely due to peptide aggregation in PBS. Previous CD studies of SP-$B_{1-25}$ in PBS indicated a concentration-dependent change in structure typical of peptide-self association (Fan et al., 1991). This aggregation phenomenon is further indicated by the characteristic ESR spectral broadening for SP-$B^*_{1-25}$ in PBS (see above), which suggested a significant population of peptide aggregates in solution.

Incorporation of SP-$B_{1-25}$ in various structure-promoting environments produced more significant "blue" shifts for Trp-9 emission. For example, suspension of SP-$B_{1-25}$ in methanol induced a "blue" shift of 15 nm for the fluorescence maxima (Table 4), consistent with Trp-9 being exposed to the more non-polar methanol molecules. Comparable "blue" shifts were also noted for this peptide in either SDS or EYL (Table 4). Here, the Trp-9 of SP-$B_{1-25}$ is inserting sufficiently into either micellar SDS or lipidic EYL to sense an hydrophobic environment comparable to that observed in methanol. However, when the SP-$B_{1-25}$ peptide was mixed with surfactant lipid dispersions of

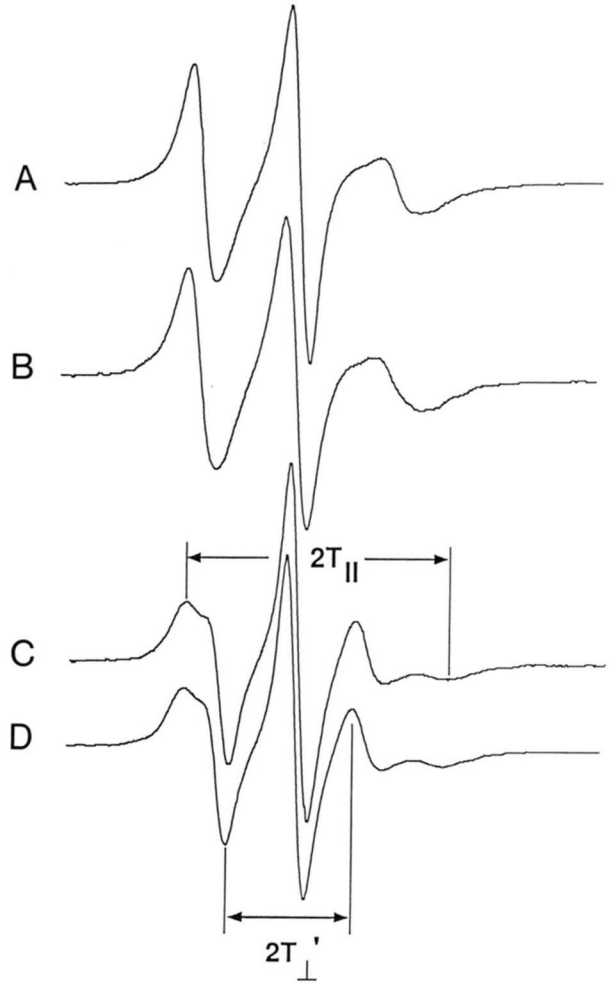


**Fig. 8.** Effects of chromium oxalate (50 mM) on the ESR spectra of EYL lipid labeled with either SP-$B^*_{1-25}$ or 5-NS (5-NS) at 39 °C. **A:** ESR spectrum of SP-$B^*_{1-25}$ labeled EYL lipid in PBS, at a peptide/lipid ratio of 1/557. **B:** ESR spectrum of SP-$B^*_{1-25}$ labeled EYL lipid in PBS with 50 mM chromium oxalate; the amplitude ($h_o$) of the spectrum is corrected for the dilution effect of the chromium oxalate addition. **C:** ESR spectrum of 5-NS labeled EYL lipid in PBS, at a probe/lipid ratio of 1/1,401. **D:** ESR spectrum of 5-NS labeled EYL lipid in PBS with 50 mM chromium oxalate; the amplitude of the spectrum is corrected for the dilution effect of the chromium oxalate addition. The outer ($2T_{\parallel}$) and inner ($2T'_{\perp}$) hyperfine splittings are determined as shown in C and D, respectively; $2T'_{\perp}$ was corrected by 0.8 Gauss (Curtain et al., 1987). *x* axis, end-to-end of spectra is equal to 90 Gauss. Probe concentrations were calculated from double-integration of the ESR spectra as described in the text.

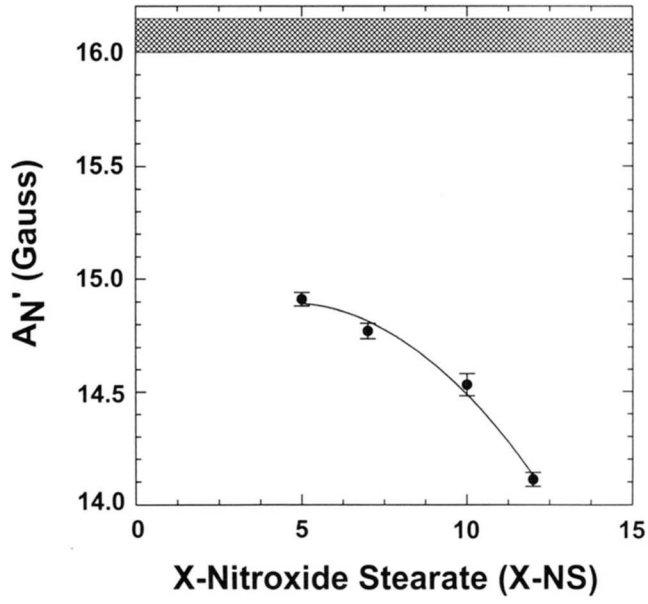


**Fig. 9.** Comparison of $a'_N$ for SP-$B^*_{1-25}$ in EYL lipid with the corresponding parameters of lipid spin-labeled with X-NS. $a'_N$ (Gauss) for the 5-NS, 7-NS, 10-NS, and 12-NS probes in EYL lipids at 34 °C were determined from $a'_N = \frac{1}{3} \cdot (T_{\parallel} + 2T_{\perp})$ G and ESR spectra as shown in Figure 8; data are presented as mean ($a'_N$) ± 1 SD, N = 4. The $a'_N$ value (±1 SD, $N = 4$) for SP-$B^*_{1-25}$ labeled EYL lipid is indicated by the cross-hatched stripe. Probe/lipid ratios for SP-$B^*_{1-25}$, 5-NS, 7-NS, 10-NS, and 12-NS were 1/1,818, 1/1,735, 1/2,018, 1/5,630, and 1/1,728. Probe concentrations were determined from double-integration of the ESR spectra as described in the text.

DPPC:unsat. PG (7:3, wt%) or Tanaka lipids (DPPC/unsat. PG/palmitic acid; 66:22:9; wt%), there was a greater "blue" shift from a solution maximum of 356 nm to 333 nm, as well as a shoulder around 344 nm. These fluorescence spectra indicate that the Trp-9 of SP-$B_{1-25}$ inserts into more hydrophobic lipid domains when the peptide is dispersed with zwitterionic/anionic lipid that is largely in the form of phospholipid bilayers.

To further examine the local environment of the Trp-9 of SP-$B_{1-25}$ in various solvent systems and lipid dispersions, the effect of steady-state solute quenching with the iodide ion or acrylamide was determined. Potassium iodide (KI) is particularly useful for probing tryptophanes nearby positively charged sites of protein (Eftink, 1991). Concentrations of KI in the range 10–200 mM rapidly quenched the fluorescence of the Trp-9 of SP-$B_{1-25}$ in all solutions and dispersions, suggesting solvent accessibility to this tryptophan residue. Examination of the quenching of Trp-9 by 10–200 mM acrylamide in solution and membrane-mimic systems (data not shown) also indicated that this residue was solvent accessible, even when in phospholipid

**Table 4.** *Tryptophan emission maxima and blue-shift for SP-$B_{1-25}$ in structure-promoting environments and surfactant lipids*

| Solvent/lipid[a] | Wavelength max[b] (nm) | Blue shift[c] (nm) |
|---|---|---|
| PBS | 353 | 3 |
| Methanol | 341 | 15 |
| SDS | 342 | 14 |
| EYL | 340 | 16 |
| DPPC/PG (unsat.) | 334 | 22 |
| Tanaka lipids | 333 | 23 |

[a] SP-$B_{1-25}$ concentration in PBS or methanol was 15 μM, and the respective SP-$B_{1-25}$/lipid ratios for SDS, EYL, DPPC/PG (unsat.), and Tanaka lipids were 1/500, 1/300, 1/300, and 1/300.

[b] Wavelength maxima reflect ±2 nm accuracy.

[c] Blue shift is taken from the maximum wavelength value (356 nm) for the free tryptophan amino acid in aqueous medium at neutral pH.

dispersions where there was a significant blue shift. Although the Trp-9 of the N-terminal SP-$B_{1-25}$ peptide samples a hydrophobic environment in the lipid headgroup (Jacobs & White, 1989; Jones & Gierasch, 1994), it is nonetheless sensitive to aqueous quenchers.

## Discussion

### *Secondary conformation of the N-terminal SP-$B_{1-25}$ peptide in structure-promoting environment and membrane mimics*

In this study, FTIR measurements of SP-$B_{1-25}$ indicated a dominant helical component in organic solvents (methanol), self-films, and lipid-peptide multilayers (Figs. 2, 3). These results are consistent with earlier CD analyses of SP-$B_{1-25}$ in structure-promoting environments (Bruni et al., 1991; Fan et al., 1991) and complement the CD measurements of the peptide in methanol detailed in the present study. FTIR measurements also show a turn component and some $\beta$-sheet and disordered conformations for SP-$B_{1-25}$ in systems that mimic surfactant dispersions used in the treatment of respiratory distress syndrome.

The experimental protocol used here for localizing secondary conformations within SP-$B_{1-25}$ was to similarly examine truncated peptides. FTIR measurements of the N-terminal segment containing the predicted $\beta$-turn tetrapeptide (SP-$B_{1-9}$) indicated that it had substantial absorbance at 1,667 $cm^{-1}$ (Fig. 4A), typical of turn conformations, as well as contributions of helix (both $3_{10}$ and $\alpha$) and some $\beta$-sheet (Table 2). Previous CD analysis of SP-$B_{1-9}$ suggests that the turn component may assume type I $\beta$-turn conformers (Perczel et al., 1993) in structure-promoting solvents, such as TFE and methanol. Although the present CD and FTIR studies of SP-$B_{1-9}$ in methanol do not indicate a unique conformation for this shortened peptide, the major conformation ($\beta$-turn) found for the 1-9 peptide probably also occurs in the parent SP-$B_{1-25}$. CD and FTIR results presented here also indicate that the C-terminal segments of SP-B (i.e., SP-$B_{15-25}$ or SP-$B_{8-25}$) principally assume helical conformations in methanol (Figs. 4, 5; Table 2). These findings support those of a recent proton 2D-NMR study of a synthetic SP-B fragment consisting of residues 11-25, confirming that leucine 14 to methionine 21 of SP-$B_{11-25}$ exists as a flexible helical conformation in methanol and the membrane-mimic SDS (Kumar, 1994). Given the inherent uncertainties of working with truncated peptides that may fray at their unprotected N-terminal and C-terminal ends, however, additional residue-specific studies on the full-length SP-$B_{1-25}$ peptide in surfactant lipid environments will be required to characterize more definitively the structure of these domains.

### *SP-$B_{1-25}$ Topography in membrane-mimic systems*

In addition to determining the secondary conformation of SP-$B_{1-25}$, an accurate topographical model for peptide insertion requires knowledge of the vertical penetration of key amino acid residues into the bilayer (or monolayer). One valuable experimental approach for obtaining such information is to record ESR spectra of peptides covalently labeled with paramagnetic reporter groups and incorporated into various environments (Altenbach & Hubbell, 1988; Gordon et al., 1992). ESR measurements indicated that SP-$B^*_{1-25}$ principally distributes in PBS as aggregated peptide (Fig. 6B), analogous to that seen with the antimicrobial peptide *cecropin AD* in hexafluoroisopropanol (10%) (Mchaourab et al., 1993). This self-association of SP-$B^*_{1-25}$ is consistent with previous CD studies (Fan et al., 1991), which indicated that SP-$B_{1-25}$ in PBS adopts a concentration-dependent, helical structure. Addition of a range of lipids to SP-$B^*_{1-25}$ altered the ESR spectra dramatically (Fig. 7), indicative of quantitative incorporation of the spin-labeled peptide by the lipids. Both the relatively high polarity (Table 3) and the absence of chromium oxalate broadening (Fig. 8) demonstrate a position for the reporter group of SP-$B^*_{1-25}$ immediately subjacent to the polar lipid headgroup.

Both endogenous Trp-9 fluorescence and susceptibility to aqueous fluorescent quenching agents (KI and acrylamide) suggest that, when SP-$B_{1-25}$ is incorporated into lipid dispersions, this residue is located in the polar head group region of the liposome bilayer. Although both the reporter group of SP-$B^*_{1-25}$ and the Trp-9 of SP-$B_{1-25}$ associate with the lipid headgroup, the latter results suggest that the tryptophan resides in the polar region of lipid bilayer ensembles that is more exposed to the aqueous compartment (Griffith et al., 1974). These results complement an earlier immunologic study (Longo et al., 1992) of SP-$B_{1-25}$ bound to liposomes that also provided information on the exposure of protein domains to the aqueous buffer. Antibodies raised to the amphipathic helical region encompassing SP-B residues Cys-8 to Gly-25 (Fan et al., 1991) showed that this sequence is accessible to the bulk aqueous solvent with SP-$B_{1-25}$ bound to surfactant liposomes (Longo et al., 1992). In this context, it should be noted that our polarized FTIR measurements indicate that the helical axis (SP-B residues 8-25) inserts in surfactant lipids at an oblique angle with respect to the surface of the film (Table 1). These observations suggest that, at mole ratios of lipid to peptide of 100:1 or greater, the amphipathic helix probably locates in the polar lipid headgroup and is accessible to the aqueous buffer.

The above structural information may be used to develop a comprehensive model for SP-$B^*_{1-25}$ interacting with lipids (Fig. 10). A refined structural model of SP-$B_{1-25}$ in the absence of lipids was formulated initially by simulated annealing in vacuo using HYPERCHEM as described in Materials and methods. The refined structure was then saved in a Brookhaven file format and imported into BIOGRAPH. The proxyl spin label with the N $\rightarrow$ O$\cdot$ radical represented as N = O was then modeled using the organic builder module of BIOGRAPH and attached to the SP-$B_{1-25}$ peptide N-terminus. The ensemble was minimized and cycled through another molecular dynamics run by fixing the peptide coordinates and allowing the spin-label structure to relax. The helical segment molecular axis was then oriented to an angle of 45 degrees with respect to the plane of the amphipathic lipid monolayer, in agreement with oriented FTIR experiments (Table 1). Limited penetration of SP-$B^*_{1-25}$ into the lipid monolayer is indicated by a polar headgroup location for both Trp-9 and the spin-labeled reporter on Phe-1, as determined from respective fluorescence and ESR studies.

The present structural studies suggest that the hydrophobicity of the N-terminal segment assists insertion of the peptide into lipid, whereas the amphipathic helix optimizes the orientation and charge specificity for interaction with specific lipids in bilayer-monolayer ensembles. Our results provide a preliminary basis for clarifying the molecular association of these types of protein sequences with surfactant lipids. More extensive inves-

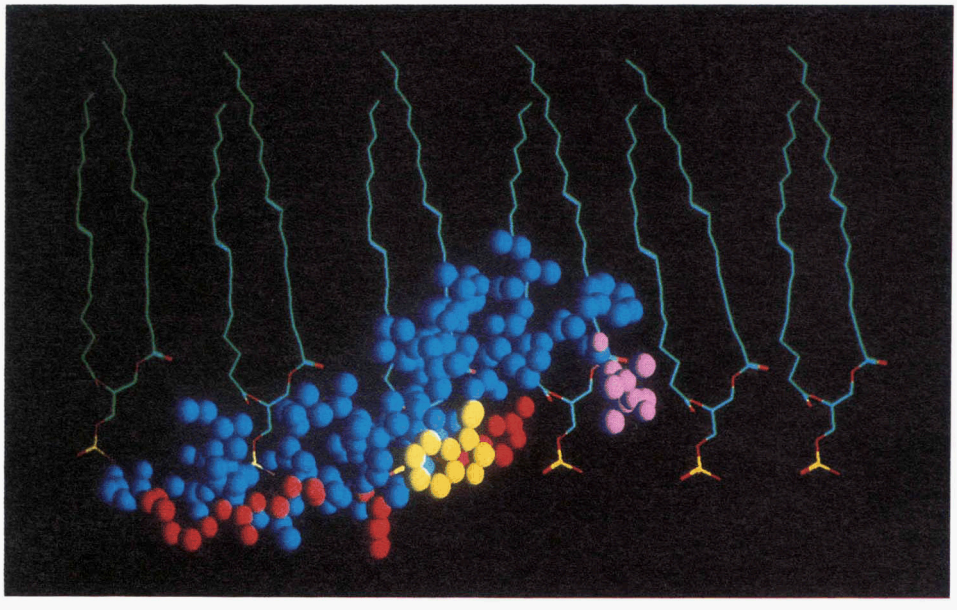

**Fig. 10.** Proposed computer graphic representation for the insertion of SP-$B^*_{1-25}$ into the lipid (PG) monolayer. The green stick structures indicate PG lipid, whereas the solid space-filling structure represents SP-$B^*_{1-25}$. The N-terminal phenylalanine (i.e., residue 1) of SP-$B^*_{1-25}$ has an attached spin-label reporter group (in purple). Tryptophan-9 is indicated in yellow, positively charged amino acid residues are in red, and hydrophobic amino acid residues are in blue. For the $\alpha$-helical component (i.e., SP-B residues 8–25), the axis is tilted at an angle ($\theta = 45$ degrees) with respect to the plane of the lipid monolayer, in agreement with oriented FTIR experiments. Limited penetration of SP-$B_{1-25}$ into the lipid monolayer is indicated by a polar headgroup location for both Trp-9 and the spin-labeled reporter of Phe-1, as determined from respective fluorescence quenching and ESR experiments.

tigations of the lipid–protein and protein–protein interactions for hydrophobic surfactant proteins, including full-length SP-B and SP-C, should permit a better understanding of defects (mutations) in surfactant function and optimization of lung surfactant in vivo.

## Materials and methods

### *Materials*

Peptide synthesis reagents including FMOC amino acid and coupling solvents were obtained from Applied Biosystems (Foster City, California). Phospholipids were from Avanti Polar Lipids (Alabaster, Alabama) and palmitic acid was obtained from Nu-Chek-Prep (Elysian, Minnesota). The covalent spin label succinimidyl 2,2,5,5-tetramethyl-3-pyrroline-1-oxyl-3-carboxylate and spin-labeled stearic acid derivatives were supplied by Molecular Probes (Eugene, Oregon). Chromium oxalate (potassium trioxalochromate) was purchased from ICN-Pharmaceuticals (Plainview, New York). All organic solvents used for sample synthesis, purification, and preparation were HPLC grade or better.

### *Solid-phase peptide synthesis, purification, and characterization*

The peptide was synthesized on a 0.25 mmol scale with an Applied Biosystems Model 431A peptide synthesizer or with an ABI Synergy synthesizer using FastMoc™ chemistry, using HBtu activation for coupling (Fields et al., 1991). A prederivatized p-benzyloxybenzl alcohol resin (Applied Biosystems) with the C-terminal glycine was used for synthesis. Double couplings were used for residues 12–18, all other residues were single coupled. The truncated N-terminal SP-B segment, residues 1–9, was synthesized with a Rink amide MBHA resin (Calbiochem-Nova, La Jolla, California) and was single coupled for all residues. Peptides representing SP-B residues 15–25 and 8–25 were N-acetylated on the resin with acetic anhydride-triethylamine in DMF.

Purification of crude peptide product was by reverse-phase HPLC with a Vydac C4-column (Vydac, Hesperia, California). The peptide was twice chromatographed using a 60-min linear gradient of 0–100% mobile phase at a flow rate of 3 mL/min to insure that no unlabeled peptide coeluted with the spin-labeled product. The starting phase was water with 0.1% TFA, and the eluting phase was 100% acetonitrile containing 0.1% TFA. The elution of the material was monitored at 250 nm so to detect the spin-labeled peptide separation on the column. Purified peptide was dried by vacuum centrifugation. Peptides were twice freeze dried from 10 mM HCl solutions to remove acetate counterions that interfere with FTIR spectral measurements. The molecular mass of the peptide was confirmed by fast atom bombardment mass spectroscopy.

### *CD spectroscopy*

CD measurements were made with either a Jasco J720 spectropolarimeter (Easton, Maryland) or an AVIV 62DS spectropolarimeter (AVIV Associates, Lakewood, New Jersey). The Jasco 720 was fitted with a SCH-1 cell holder to minimize light scat-

tering artifacts, and the temperature of the sample was controlled using the water-jacketed Jasco cuvette accessory coupled to a Neslab constant temperature bath. The AVIV 62DS was fitted with a thermoelectric temperature controller. Lipid–peptide dispersions in 0.1-mm light path demountable cells were scanned from 250 nm to 195 nm at a rate of 20 (or 10) nm/min and a sample interval of 0.2 nm. The instrument was routinely calibrated with (+)-10-camphorsulfonic acid (1 mg/mL) and a 1-mm-pathlength cell (Johnson, 1990), and the ellipticity expressed as the mean residue ellipticity, $[\theta]_{MRE}$ (deg cm$^2$ dmol$^{-1}$). Peptide sample concentrations were determined from the UV absorbance at 280 nm using an extinction coefficient based on aromatic amino acid residues (Gill & von Hippel, 1989) and by quantitative amino acid analysis (UCLA Microsequencing Facility, Los Angeles, California). The percentage of $\alpha$-helix conformation in the peptide was estimated using the formalism of Chen et al. (1974). This approach assumes the maximum theoretical ellipticity for a given peptide or protein at 222 nm may be derived from the number of amino acid residues $n$, and the ellipticity at 222 nm of a helix of infinite length described by Equation 1.

$$\% \ \alpha\text{-helix} = \frac{[\theta]_{MRE222}}{-39{,}500(1 - (2.57/n))} \text{ deg cm}^2 \text{ dmol}^{-1} \quad (1)$$

*FTIR spectroscopy*

Infrared spectra were recorded at 38 °C on a Mattson Research Series FTIR spectrometer with a DTGS detector. Peptides in methanol solution were measured in $CaF_2$-cm-pathlength cells. Spectra were averaged over 64 scans at a resolution of 2 cm$^{-1}$. Peptide self-films were prepared by air dying peptide solutions (in methanol or hexafluoroisopropanol) onto 50 × 20 × 3 mm 45 degree ATR crystal (Spectra Tech, Stamford, Connecticut). Lipid–peptide films were also air-dried onto the ATR crystal with the following procedure. Peptides were first aliquoted from methanol stock solution, and dried in a microfuge vial using a vacuum concentrator. The dry peptide was then mixed with a solution of isopropanol:water (9:1, v:v) containing the lipid, and the mixture was applied to the ATR crystal to form multilayers. The ATR crystal with the lipid–peptide film was sandwiched in a chamber fabricated from black anodized aluminum (Matsuzaki et al., 1991), and mounted on the model 304 variable ATR (Spectra Tech) with a Minco heater strip controlled with an Omega (Stamford, Connecticut) temperature regulator. The lipid–peptide sample was then hydrated for 2 h by passing nitrogen $D_2O$ vapor through ports in the cell body. Spectra were averaged from 64 scans at a gain of 4 and a spectral resolution of 2 cm$^{-1}$. The IR range was typically scanned from 4,000 wavenumbers (cm$^{-1}$) to 500 wavenumbers (cm$^{-1}$), which includes both the conformational bands (Amide I, II, and II) of the peptide, as well as the lipid acyl chain stretching modes [$CH_2$-$CH_2$, ~2,850 wavenumbers (cm$^{-1}$)]. The orientation of the helical axis of the peptide relative to the lipid multilayers was assessed by placing a gold wire grid polarizer (Perkin-Elmer) in the infrared beam parallel and perpendicular to the ATR crystal surface with oriented lipid–peptide film. Acyl chain orientations for lipid–peptide films spread onto the germanium substrate were estimated from polarization measurements of the $CH_2$ asymmetric stretching frequency 2,850 cm$^{-1}$ (Okamura et al., 1990). The dichroic ratio ($R_{ATR}$), an index of the mean acyl chain orientation in the film, was determined by the ratio of the absorption of linearly polarized light parallel ($A_\parallel$) and perpendicular ($A_\perp$) to the plane of incidence ($R_{ATR} = A_\parallel/A_\perp$).

The relative contribution of the various peptide conformations in the lipid film was estimated from analysis of the amide I bands of the sample. The spectrum of the lipid film without peptide was subtracted from that of samples with peptide associated with lipid. The amounts of helix, turn, $\beta$-structure, and disordered conformations was determined by Fourier self-deconvolution for band narrowing and area calculations of component peaks calculated with curve fitting software supplied by Mattson and based on procedures described by Kauppine et al. (1981).

*ESR spectrometry*

The N-terminus of SP-$B_{1-25}$ was spin labeled (i.e., SP-$B^*_{1-25}$; Fig. 1) by de-FMOCing the N-terminal residue while the peptide was still on the resin, using 20% piperidine in N-methylpyrrolidone, followed by dimethylformamide and dichloromethane washes. The peptide was then labeled with excess succinimidyl 2,2,5,5, tetramethyl 3-pyroline spin label in acetonitrile:bicarbonate buffer (10 mM, pH 8.3) for 2 h. SP-$B^*_{1-25}$ was isolated with reverse-phase HPLC, and the purity assessed with FAB mass spectroscopy and quantitative amino acid analysis.

Spin-labeled SP-$B^*_{1-25}$ stock solutions were prepared by dissolving SP-$B^*_{1-25}$ in 100% methanol at 2.73 × 10$^{-4}$ mol/L. Before lipid addition to SP-$B^*_{1-25}$, small volumes of the peptide probe solution were added to plastic vials and dried by centrifuging under vacuum. Aliquots (100 $\mu$L) of PBS, pH 7.4, or lipids suspended in PBS were then added and hand-vortexed for several minutes at room temperature. Spin-labeled samples (25-$\mu$L aliquots) were drawn into 50-$\mu$L capillary pipettes that were subsequently heat-sealed at one end. The sealed capillaries were then inserted into a special holder (Gaffney, 1974; Curtain et al., 1987), and this assembly was then introduced into the Dewar of the variable temperature regulator of the ESR spectrometer.

The extent of probe incorporation was tested by comparing the amount of probe added to the lipid solution (i.e., mol probe/mol lipid "wt") with the paramagnetic spins observed in the microwave cavity (i.e., mol probe/mol lipid "spins"). Spins were calculated (Gordon et al., 1985; Curtain et al., 1987) from the ratio of the double-integrated spectrum of probe-labeled agent solution with that of the Varian Strong-Pitch [0.1% pitch, with 3 × 10$^{15}$ spins in 5.5 mm]. Similar calculations were performed to calculate the % SP-$B^*_{1-25}$ uptake in methanol and PBS solutions.

The ESR spectra were recorded with a Varian E-104A spectrometer equipped with a variable temperature accessory. For computer analysis, ESR spectra were first scanned with a Hewlett-Packard Scanjet IIC at 100 dpi, and then digitized into 2,300 points with UNGRAPH (Biosoft, Oxford, UK). Computer manipulations of the experimental spectra, such as signal averaging and integrations, were performed using SpectraCalc Version 2.23 (Galactic Industries Corp., Salem New Hampshire).

*Evaluation of the flexibility and polarity of lipid-incorporated SP-$B^*_{1-25}$ or NS probes*

Two distinct motional regimes were noted for the probe molecules used here. For SP-$B^*_{1-25}$ in 100% methanol, or with lip-

ids suspended in PBS, pH 7.4, the motion of the probe attached to SP-$B_{1-25}$ is nearly isotropic. A rotational correlation time ($\tau_R$) may be calculated that provides an empirical parameter sensitive to motion in the region probed by the spin label (Keith et al., 1974):

$$\tau_R = 6.5 \times 10^{-10} \cdot \Delta H_o [(h_o/h_{-1})^{1/2} - 1] \quad (2)$$

where $\Delta H_o$ is equal to the peak-to-peak distance of the central band (Fig. 6A), and $h_o$ and $h_{-1}$ are measured as in Figure 6A. Equation 2 is valid for $\tau_R \sim 10^{-10}$ s. The $a'_N$ in Gauss is sensitive to the polarity of the environment of the probe and is measured as shown in Figure 6A; increases in $a'_N$ indicate a more polar environment.

For motional ranges where the spin-labeled, nitroxide stearic acid probes (NS) exhibit anisotropic rotation and restricted flexibility (e.g., Fig. 8C,D), the order parameter $S$ may be used to assess flexibility:

$$S = \frac{(T_\parallel - T_\perp)}{(T_{zz} - T_{xx})} \frac{(a_N)}{(a'_N)} \quad (3)$$

where $T_\parallel$ and $T_\perp$ for the incorporated spin probe are two phenomenologic hyperfine splitting parameters in the effective Hamiltonian theory (Hubbell & McConnell, 1971), and can be determined experimentally as shown in Figure 8C and D. The other two hyperfine splitting parameters, $T_{xx}$ and $T_{zz}$, in Equation 3 are the principal elements of the real hyperfine splitting tensor (**T**) in the spin Hamiltonian of the probe system, which can be measured from corresponding single-crystal ESR spectra. According to earlier review (Gaffney, 1974; Curtain et al., 1987), ($T_{xx}$, $T_{zz}$) is equal to (6.1, 32.4) G, and $a'_N$ and $a_N$ are the isotropic hyperfine coupling constants for the probe given by $a'_N = \frac{1}{3} \cdot (T_\parallel + 2T_\perp)$ G and $a_N = \frac{1}{3} \cdot (T_{zz} + 2T_{xx})$ G, respectively. For the same solvent polarity, $a'_N$ and $a_N$ become identical because of the general principle for tensor transformations in quantum mechanics. Increases in $a'_N$ indicate a more polar environment for the probe.

If experimentally determined low probe concentrations are used (Sauerheber et al., 1977), $S$ is sensitive to the flexibility of the incorporated probe. These order parameters may assume values between 0 and 1, with the extremes indicating that the probe samples fluid and motionally restricted environments, respectively. $S$, which requires both splittings, corrects for small polarity differences between the agent environment and the reference crystal.

### *Tryptophan fluorescence spectroscopy*

Steady-state fluorescence spectra of the tryptcphan containing SP-B sequence in lipid–peptide dispersions were made using a Perkin-Elmer LS-5B Luminescence spectrometer at 38 °C. The sample was measured using a front surface fluorescence-luminescence accessory (Perkin-Elmer) that minimizes dispersion light scattering artifacts (Waring et al., 1989).

### *Molecular modeling*

The amino-terminal peptide of SP-B (SP-$B_{1-25}$) was modeled with HYPERCHEM software version 3.0 (Autocad, Sausalito, California) on either a Dell 90 MHz computer or a Silicon-Graphic Iris Indigo workstation (Drew-RCMI Epistat core facility). Energy minimizations and molecular dynamics were performed using the AMBER force field within the HYPERCHEM software environment. Torsional angles derived from energy minimizations and dynamics of the SP-$B_{1-25}$ were obtained using Chem-Plus™ (Hypercube, Inc., Waterloo, Ontario) extension of HYPERCHEM. Type III $\beta$-turn ($3_{10}$ helix) dihedrals were used for residues 1–7, whereas an $\alpha$-helical motif was applied to residues 8–21. All other residue torsionals were considered to be random. The structure was then energy minimized by Polak–Ribiere conjugate gradient minimization to an apparent minimum (0.1 kcal/mol). The structure was then relaxed by simulated annealing in vacuo. The temperature was increased from 300 to 900 K using a step of 5 fs for 30 ps. The simulated heating was then followed by 30 ps of molecular dynamics at 900 K and cooled to 300 K for 50 ps with a time step of 5 fs. The relaxed structure was then optimized by conjugate gradient minimization. The refined structure had dihedrals that corresponded to helix ($-130 \le \phi \le 10$; $-90 \le \psi \le -10$) for residues 5–19; residues 3–4, 20–22 had torsional angles more characteristic of $\beta$-sheet ($-180 \le \phi \le -50$; $80 \le \psi \le 180$), whereas all other dihedrals belonged to no specific conformational class (i.e., random). The refined structure was then saved in a Brookhaven file format and imported into BIOGRAF version 3.2.1 (Molecular Simulations, Walthan, Massachusetts) for final presentation in the lipid monolayer, assembled from the BIOGRAF lipid library.

## Acknowledgments

We thank Dr. Larry Vickery (UC Irvine) for use of the Jasco J-720 CD spectrometer and Dr. James Bowie (UCLA) for use of the AVIV 62DS spectropolarimeter. We acknowledge Conrado Savilla III and John Racs for their help with the synthesis and cleavage of the spin-labeled SP-B peptides. Special thanks to Dr. Maria Mas for access to the Beckman City of Hope Molecular Modeling Facility, and to Dr. Mark Sherman for assistance in modeling the peptide–lipid ensemble in the BIOGRAF environment. We are grateful to Dr. Tim Wiedman for sharing prepublication, residue-specific 2D NMR data on a synthetic peptide comprising the N-terminal helical segment of SP-B. We also thank the reviewers, Mike Lipp, and Ka Yee Lee for their helpful comments on the manuscript. This study was supported by NIH grant HL 40666 (H.W.T., A.W., L.G.), HL 55534 and RCMI G12 RR 3026 (A.W., L.G.), and HL 51177-02 (J.J.Z.). The ABI 431A peptide synthesizer was acquired by an NIH small equipment grant GM 50483 (A.W., L.G.).

## References

Altenbach C, Hubbell WL. 1988. The aggregation state of spin-labeled melittin in solution and bound to phospholipid membranes: Evidence that membrane-bound melittin is monomeric. *Proteins Struct Funct Genet 3*:230–242.

Baatz JE, Elledge B, Whitsett JA. 1990. Surfactant protein SP-B induces ordering at the surface of model membrane bilayers. *Biochemistry 29*:6714–6720.

Brauner JW, Mendelsohn R, Prendergast FG. 1987. Attenuated total reflectance Fourier transform infrared studies of the interactions of melittin, two fragments of melittin, and $\alpha$-hemolysin with phosphatidylcholines. *Biochemistry 26*:8151–8158.

Bruni R, Taeusch HW, Waring AJ. 1991. Surfactant protein B: Lipid interactions of synthetic peptides representing the amino-terminal amphipathic domain. *Proc Natl Acad Sci USA 88*:7451–7455.

Chen YH, Yang JT, Chau KH. 1974. Determination of the helix and $\beta$ form of proteins in aqueous solution by circular dichroism. *Biochemistry 13*: 3350–3359.

Curstedt T, Johansson J, Persson P, Eklund A, Robertson B, Lowenadler B, Jörnvall H. 1990. Hydrophobic surfactant-associated polypeptides: SP-C is a lipopeptide with two palmitoylated residues whereas SP-B lacks

covalently linked fatty acid groups. *Proc Natl Acad Sci USA 87*: 2985–2989.

Curtain CC, Looney FD, Gordon LM. 1987. Electron spin resonance spectroscopy in the study of lymphoid cell receptors. *Methods Enzymol 150*:418–446.

Eftink MR. 1991. Fluorescence quenching: Theory and application. In: Lakowicz J, ed. *Topics in fluorescence spectroscopy, vol 2*. New York: Plenum Press. pp 53–120.

Fan BR, Bruni R, Taeusch HW, Findlay R, Waring A. 1991. Antibodies against synthetic amphipathic helical sequences of surfactant protein SP-B detect a conformational change in the native protein. *FEBS Lett 282*: 220–224.

Fields CG, Lloyd DH, Macdonald RL, Ottenson KM, Noble RL. 1991. HBTU activation for automated Fmoc solid-phase peptide synthesis. *Peptide Res 4*:95–101.

Fiori WR, Millhauser GL. 1995. Exploring the $3_{10}$-helix ⇌ $\alpha$ helix equilibrium with double label electron spin resonance. *Biopolymers (Peptide Sci) 37*:243–250.

Folch J, Lees M, Sloane-Stanley GH. 1957. A simple method for the isolation and purification of total lipids from animal tissues. *J Biol Chem 226*:497–505.

Gaffney BJ. 1974. Spin-label measurements in membranes. *Methods Enzymol 32*:161–198.

Gill SC, von Hippel PH. 1989. Calculation of protein extinction coefficients from amino acid sequence data. *Anal Biochem 182*:319–326.

Goormaghtigh E, Cabiaux V, Ruysschaert JM. 1990. Secondary structure and dosage of soluble and membrane proteins by attenuated total reflection Fourier-transform infrared spectroscopy on hydrated films. *Eur J Biochem 193*:409–420.

Gordon LM, Curtain CC, Zhong YC, Kirkpatrick A, Mobley PW, Waring AJ. 1992. The amino terminal peptide of HIV-1 glycoprotein 41 interacts with human erythrocyte membranes: Peptide conformation, orientation and aggregation. *Biochim Biophys Acta 1139*:257–274.

Gordon LM, Looney FD, Curtain CC. 1985. Spin probe clustering in human erythrocyte ghosts. *J Membrane Biol 84*:81–95.

Griffith OH, Dehlinger PJ, Van SP. 1974. Shape of the hydrophobic barrier of phospholipid bilayers. Evidence for water penetration in biological membranes. *J Membrane Biol 15*:159–192.

Hollosi M, Majer ZS, Ronai AZ, Magyar A, Medzihradszky K, Holly S, Perczel A, Fasman GD. 1994. CD and fourier transform IR spectroscopic studies of peptides II. Detections of B-turns in linear peptides. *Biopolymers 34*:177–185.

Hubbell WL, McConnell HM. 1971. Molecular motion in spin-labeled phospholipids and membranes. *J Am Chem Soc 93*:314–326.

Jacobs RE, White SH. 1989. The nature of the hydrophobic binding of small peptides at the bilayer interface: Implications for the insertion of transbilayer helices. *Biochemistry 28*:3421–3437.

Johnson WC Jr. 1990. Protein secondary structure and circular dichroism: A practical guide. *Proteins Struct Funct Genet 7*:205–214.

Jones JD, Gierasch LM. 1994. Effect of charged residue substitutions on the membrane-interactive properties of signal sequences of the *Escherichia coli* LamB protein. *Biophys J 67*:1534–1545.

Jost PC, Griffith OH. 1978. The spin-labeling technique. *Methods Enzymol 49*:369–418.

Kauppine J, Moffatt D, Mantsch H, Cameron D. 1981. Fourier self-deconvolution: A method for resolving intrinsically overlapped bands. *Appl Spectroscopy 35*:272–278.

Keith AD, Horvat D, Snipes W. 1974. Spectral characterization of $^{15}N$ spin labels. *Chem Phys Lipids 13*:49–62.

Knowles PF, Marsh D, Rattle HWE. 1976. *Magnetic resonance of biomolecules*. New York: Wiley.

Kumar S. 1994. Conformational analysis of a synthetic fragment of lung surfactant apolipoprotein B [thesis]. University of Minnesota, Minneapolis, Minnesota 55455.

Lipp MM, Lee KYC, Zasadzinski JA, Waring AJ. 1996. Phase and morphology changes induced by SP-B protein and its amino-terminal peptide in lipid monolayers. *Science* (in press).

Longmuir KJ, Waring AJ, Haynes S. 1992. Lipid bilayer fusion promoted by a synthetic N-terminal segment of surfactant protein B. *Biophys J 61*:2873 [Abstr.]

Longo ML, Bisagno AM, Zasadzinski JAN, Bruni R, Waring A. 1993. A function of lung surfactant protein SP-B. *Science 261*:453–456.

Longo ML, Waring A, Zasadzinski JAN. 1992. Lipid bilayer surface association of lung surfactant protein SP-B, amphipathic segment detected by flow immunofluorescence. *Biophys J 63*:760–773.

Matsuzaki K, Shioyama T, Okamura E, Umemura J, Takenaka T, Takaishi Y, Fujita T, Miyajima K. 1991. A comparative study on interactions of $\alpha$-aminoisobutyric acid containing antibiotic peptides, trichopolyn I and hypelcin A with phosphatidylcholine bilayers. *Biochim Biophys Acta 1070*:419–428.

Mchaourab HS, Hyde JS, Feix JB. 1993. Aggregation state of spin-labeled cecropin AD in solution. *Biochemistry 32*:11895–11902.

Miick SM, Martiez GV, Fiori WR, Todd PA, Millhauser GL. 1992. Short alanine-based peptides may form $3_{10}$ and $\alpha$ helices in aqueous solution. *Nature 359*:653–655.

Morrow MR, Pérez-Gil J, Simatos G, Boland C, Stewart J, Absolom D, Sarin V, Keough KMW. 1993. Pulmonary surfactant-associated protein SP-B has little effect on acyl chains in dipalmitoylphosphatidylcholine dispersions. *Biochemistry 32*:4397–4402.

Okamura E, Umemura J, Takenaka T. 1990. Orientation studies of hydrated dipalmitoylphosphatidylcholine multilayers by polarized FTIR-ATR spectroscopy. *Biochim Biophys Acta 1025*:94–98.

Oosterlaken-Dijksterhuis MA, Haagsman HP, van Golde LLM, Demel RA. 1991. Characterization of lipid insertion into monomolecular layers mediated by lung surfactant proteins SP-B and SP-C. *Biochemistry 30*: 10965–10971.

Oosterlaken-Dijksterhuis MA, van Eijk M, van Golde LMG, Haagsman HP. 1992. Lipid mixing is mediated by the hydrophobic surfactant protein SP-B but not by SP-C. *Biochim Biophys Acta 1110*:45–50.

Perczel A, Hollosi M, Sandor P, Fasman G. 1993. The evaluation of type I and type II B-turn mixtures. Circular dichroism, NMR and molecular dynamics studies. *Int J Peptide Protein Res 41*:223–236.

Pérez-Gil J, Casals C, Marsh D. 1995. Interactions of hydrophobic lung surfactant proteins SP-B and SP-C with dipalmitoylphosphatidylcholine and dipalmitoylphosphatidylglycerol bilayers studied by electron spin resonance spectroscopy. *Biochemistry 34*:3964–3971.

Pérez-Gil J, Cruz A, Casals C. 1993. Solubility of hydrophobic surfactant proteins in organic solvent/water mixtures. Structural studies on SP-B and SP-C in aqueous organic solvents and lipids. *Biochim Biophys Acta 1168*:261–270.

Possmayer F. 1988. A proposed nomenclature for pulmonary surfactant-associated proteins. *Am Rev Respir Dis 138*:990–998.

Sauerheber RD, Gordon LM, Crosland RD, Kuwahara MD. 1977. Spin-label studies on rat liver and heart plasma membranes: Do probe-probe interactions interfere with the measurement of membrane properties? *J Membrane Biol 31*:131–169.

Seelig J, Hasselbach W. 1971. A spin label study of sarcoplasmic vesicles. *Eur J Biochem 21*:17–21.

Susi H, Byler DM. 1986. Calculation of the secondary structure of protein by deconvoluted FTIR spectra. *Biopolymers 25*:459–487.

Takahashi A, Waring A, Amirkhanian J, Fan R, Taeusch W. 1990. Structure-function relationships of bovine pulmonary surfactant proteins: SP-B and SP-C. *Biochim Biophys Acta 1044*:43–49.

Vandenbussche G, Clercx A, Clercx M, Curstedt T, Johansson J, Jörnvall H, Ruysschaert J. 1992. Secondary structure and orientation of the surfactant protein SP-B in a lipid environment. A Fourier transform infrared spectroscopy study. *Biochemistry 31*:9169–9176.

Vincent JS, Revak SD, Cochrane CG, Levin IW. 1991. Raman spectroscopic studies of model human pulmonary surfactant systems: Phospholipid interactions with peptide paradigms for the surfactant protein SP-B. *Biochemistry 30*:8395–8401.

Vincent JS, Revak SD, Cochrane CG, Levin IW. 1993. Interactions of model human pulmonary surfactants with mixed phospholipid bilayer assembly: Raman spectroscopic studies. *Biochemistry 32*:8228–8238.

Waring AJ, Taeusch HW, Bruni R, Amirkhanian J, Fan B, Stevens R, Young J. 1989. Synthetic amphipathic sequences of surfactant protein-B mimic several physicochemical and in vivo properties of native pulmonary surfactant proteins. *Peptide Res 2*:308–313.

Wiedman T. 1991. The effect of lung surfactant apoproteins B/C in the chemical shift anisotropy on sn 2(1-13c)-DPPC. *Biophys J 59*:624A. [Abstr.]